Hybrid Precoding for Millimeter Wave Multiuser Massive MIMO Systems with Low-Resolution DACs

Yajing Guo, Yunliang Zhang, Shuaifei Chen, Jiakang Zheng, and Jiayi Zhang
School of Electronic and Information Engineering, Beijing Jiaotong University, Beijing 100044, China

***Abstract*—To reduce the hardware cost and power consumption in millimeter wave (mmWave) multiuser massive multiple-input multiple-output (MIMO) systems, a quantized hybrid transmit model with low-resolution digital-to-analog converters (DACs) is introduced. A correlation-based hybrid precoding algorithm is proposed as an attractive low-complexity approach for the considered system. Using the Bussgang theorem and the additive quantization noise model (AQNM), we derive the asymptotic downlink achievable rate expressions. The rate loss caused by low-resolution DACs shows negligible quantization distortion at low power regime. Numerical results demonstrate the superiority of the proposed algorithm over other algorithms in terms of the rate performance.**

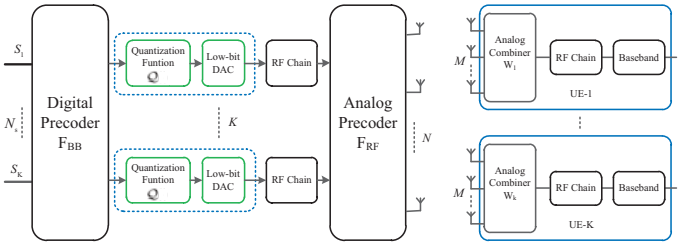

Fig. 1. Hybrid precoding for mmWave multiuser massive MIMO systems with low-resolution DACs and full-connected architecture.

I. Introduction

With several hundreds of antenna elements at the base station (BS), multiuser massive multiple-input multiple-output (MIMO) systems can provide superior performance in the spectral and energy efficiency with simple signal processing on the same time-frequency resource [1]–[4]. Since each antenna requires a radio-frequency (RF) chain with two digital-to-analog converters (DACs) at the transmitter, the hardware cost and power consumption significantly increase in massive MIMO systems. To make massive MIMO systems practical, two energy-efficiency approaches have been proposed [5]. One is to employ hybrid analog/digital (A/D) architecture [6]. Alternatively, each RF chain is connected with low-resolution DACs [7].

Recently, a combination of hybrid A/D architecture and low-resolution DACs has attracted much research interest due to its potential cost- and energy-efficiency. The authors in [8] characterized the performance of the downlink massive MIMO with transceiver quantization based on the Bussgang theorem. An extension to hybrid systems employing low-resolution DACs/ADCs at transceiver was proposed in [9], where only a single-user MIMO system model has been considered. In [10], a one-bit precoding solution was proposed to minimize the detection error probability of all users. At the cost of an increased computational complexity, novel nonlinear precoding algorithms were proposed to increase the performance for the case of 1-bit DACs [11]. However, both works focus on the special case of 1-bit DACs and sub-6 GHz spectrum. The mmWave band can provide large bandwidths and allow for high date rate. The sparse propagation characteristics of mmWave channels are totally different from sub-6 GHz channels.

In this paper, we propose a low-complexity hybrid precoding algorithm of quantized mmWave multiuser massive MIMO systems with low-resolution DACs. The contributions of this paper are as follows:

- A low-complexity hybrid precoding algorithm has been proposed by correlation-based method for the analog precoder and zero-forcing (ZF) for the digital precoder.
- We derive achievable rate expressions based on the Bussgang theorem and the additive quantization noise model (AQNM), respectively. The effect of DAC quantization bits on the achievable rate is assessed in detail.

Notation: We use bold lower case $\mathbf{a}$ and upper case $\mathbf{A}$ to denote vectors and matrices, respectively. The notation $\mathbf{A}_{i,j}$ is the entry on the ith row and jth column element of $\mathbf{A}$. The conjugate, the transpose, and the conjugate transpose of $\mathbf{A}$ are represented by $\mathbf{A}^*$, $\mathbf{A}^T$, and $\mathbf{A}^H$, respectively. Moreover, $\det(\mathbf{A})$ and $\|\mathbf{A}\|_F$ denote the determinant and Frobenius norm of $\mathbf{A}$. Expectation is denoted by $\mathbb{E}\{\cdot\}$. Finally, $\mathrm{diag}(\mathbf{A})$ means creating a diagonal matrix whose elements are diagonal elements from matrix $\mathbf{A}$.

II. System and Channel Model

As mmWave operates in the wide bandwidths, the conventional digital precoding with a large number of antennas, the corresponding RF chains will bring high energy consumption. To solve this problem, the hybrid analog and digital precoding has been proposed [12]. Since we focus on the hybrid precoder, perfect channel state information (CSI) is assumed known at the BS. In order to alleviate the challenges of high hardware cost and power consumption, we adopt a smaller number of RF chains and hybrid precoding, where the precoder processing is partitioned into large-dimensional analog processing with lower-dimensional digital processing, respectively. Moreover, the full-connected architecture, where each RF chain is connected to all antennas through phase shifters, is adopted. This is due to the reason that the full-connected architecture is more spectral-efficiency at the cost of more phase shifters [13].

This work was supported in part by National Natural Science Foundation of China under Grants 61971027, in part by Beijing Natural Science Foundation under Grants 4182049 and L171005, and in part by the ZTE Corporation.

978-1-7281-5207-3/20/$31.00 ©2020 IEEE

As illustrated in Fig. 1, the BS communicates with K users (UEs) via only K streams. Thus, each UE can only receive one data stream. The BS employs N transmit antennas and N_{RF} RF chains with low-resolution DACs, while each UE is assumed to have M antennas and one RF chain. Therefore, the number of UE and the number of RF chains are subject to $K \leq N_{\mathrm{RF}}$. For simplicity, we assume $K = N_{\mathrm{RF}}$ [14].

For the downlink transmission, the BS first performs a baseband digital precoder $\mathbf{F}_{\mathrm{BB}} = \left[\mathbf{f}_1^{bb}, \mathbf{f}_2^{bb}, \ldots, \mathbf{f}_K^{bb}\right] \in \mathbb{C}^{K\times K}$, where $\mathbf{f}_k^{bb} \in \mathbb{C}^{K\times 1}$ represents a precoding vector corresponding to the kth UE; then, the BS applies an RF analog precoder $\mathbf{F}_{\mathrm{RF}} \in \mathbb{C}^{N\times K}$. The transmit signal vector is given by

$$\mathbf{x} = \sum_{i=1}^{K} \mathbf{F}_{\mathrm{RF}} \mathcal{Q}\left(\mathbf{f}_k^{bb} s_k\right) \tag{1}$$

where the digital baseband signal $\mathbf{s} = [s_1, s_2, \ldots, s_K]^T$ is assumed to be independent for different UEs with zero-mean and unit power, such as $\mathbb{E}\left\{\mathbf{s}\mathbf{s}^H\right\} = \mathbf{I}_K$. $\mathcal{Q}(\cdot)$ represents a nonlinear scalar quantization function at the transmitter, which separately quantizes the real and imaginary parts of the signal. The signal received at the antennas of the kth UE is given by

$$\mathbf{y}_k = \mathbf{H}_k \mathbf{x} + \mathbf{n}_k, \tag{2}$$

where $\mathbf{H}_k \in \mathbb{C}^{M\times N}$ denotes the mmWave channel matrix from the BS to the kth UE, and $\mathbf{n}_k \sim \mathcal{CN}\left(0, \sigma_n^2 \mathbf{I}\right)$ denotes the additive white Gaussian noise (AWGN) vector with zero mean and variance σ_n^2. After the analog combining, we have

$$\begin{aligned} r_k = {} & \mathbf{w}_k^* \mathbf{H}_k \mathbf{F}_{\mathrm{RF}} \mathcal{Q}\left(\mathbf{f}_k^{bb} s_k\right) \\ & + \mathbf{w}_k^* \mathbf{H}_k \mathbf{F}_{\mathrm{RF}} \sum\nolimits_{u\neq k}^{K} \mathcal{Q}\left(\mathbf{f}_u^{bb} s_u\right) + \mathbf{w}_k^* \mathbf{n}_k, \end{aligned} \tag{3}$$

where $\mathbf{w}_k \in \mathbb{C}^{1\times M}$ is the analogy combiner vector at the kth UE. In addition, the analog precoders and combiners are implemented with a network of variable analog phase shifters, which only adjust the signal phase. From (3), the signal-to-interference-plus-noise ratio (SINR) at the kth UE is given by

$$\mathrm{SINR}_k = \frac{\left|\mathbf{w}_k^* \mathbf{H}_k \mathbf{F}_{\mathrm{RF}} \mathcal{Q}\left(\mathbf{f}_k^{bb} s_k\right)\right|^2}{\sum_{u\neq k}^{K} \left|\mathbf{w}_k^* \mathbf{H}_k \mathbf{F}_{\mathrm{RF}} \mathcal{Q}\left(\mathbf{f}_u^{bb} s_u\right)\right|^2 + \sigma_n^2 |\mathbf{w}_k^*|^2}. \tag{4}$$

With the help of the worst-case uncorrelated additive noise theorem, the achievable rate R_k for the kth UE is given by

$$R_k = \log_2\left(1 + \mathrm{SINR}_k\right). \tag{5}$$

Due to the high free-space path loss and limited scattering, mmWave channel has only a few dominant multipaths and no longer obey the conventional Rayleigh fading [14], [15]. To characterize the mmWave MIMO channel, we adopt the extended geometric Saleh-Valenzuela channel model [15]. Therefore, the mmWave channel matrix $\mathbf{H}_k$ from BS to the kth UE can be depicted as

$$\mathbf{H}_k = \sqrt{\frac{NM}{L_k}} \sum_{k=1}^{L_k} \alpha_k \mathbf{a}_r\left(\phi_k^{\mathrm{r}}, \theta_k^{\mathrm{r}}\right) \mathbf{a}_t^*\left(\phi_k^{\mathrm{t}}, \theta_k^{\mathrm{t}}\right), \tag{6}$$

where L_k denotes the number of propagation paths in $\mathbf{H}_k$, $\alpha_k \sim \mathcal{CN}\left(0, \sigma_{\alpha,k}^2\right)$ denotes the complex gain of the kth propagation path, which is assumed to be identically and independently distributed (i.i.d.) complex Gaussian distribution. $\sqrt{NM/L_k}$ is the normalization factor such that $\mathbb{E}\left\{\|\mathbf{H}_k\|_F^2\right\} = NM$. In addition, $(\phi_k^{\mathrm{r}}, \theta_k^{\mathrm{r}})$ and $(\phi_k^{\mathrm{t}}, \theta_k^{\mathrm{t}})$ stand for (azimuth and elevation) angles of arrival and departure (AoAs and AoDs), respectively. The vectors $\mathbf{a}_r\left(\phi_k^{\mathrm{r}}, \theta_k^{\mathrm{r}}\right)$ and $\mathbf{a}_t\left(\phi_k^{\mathrm{t}}, \theta_k^{\mathrm{t}}\right)$ represent the normalized receive and transmit array response vectors, respectively. The array geometries are feasible for arbitrary array geometries.

III. Hybrid Precoding Design

In this section, we design the RF analog precoders $\mathbf{F}_{\mathrm{RF}}$ and digital precoders $\mathbf{F}_{\mathrm{BB}}$ at the BS, and the RF analog combiners $\mathbf{w}_k$ at the UE to maximize the sum-rate of the quantized mmWave multiuser massive MIMO system.

A. Analog Precoding Design

First, we aim to design the analog precoding and combiner to harvest the large array gain. Therefore, both analog precoder and combiner are jointly designed to maximize the desired signal power of each UE. It reduces to a beamforming design problem between the BS and single-user. Since analog precoder and combiner are implemented by analog phase shifters, the entries of $\mathbf{w}_k$ and $\mathbf{F}_{\mathrm{RF}}$ are limited to have the same norm. The optimization problem is to maximize the receive signal power of each UE as

$$\max_{\mathbf{w}_k, \mathbf{F}_{\mathrm{RF}}} \|\mathbf{w}_k^* \mathbf{H}_k \mathbf{F}_{\mathrm{RF}}\| \tag{7}$$

where $\mathbf{F}_{\mathrm{RF}} = \left[\mathbf{f}_1^{rf}, \mathbf{f}_2^{rf}, \ldots, \mathbf{f}_K^{rf}\right]$. We normalize the entries to satisfy $\left|\mathbf{f}_k^{rf}\right| = \frac{1}{\sqrt{N}}$ and $\left|(\mathbf{w}_k)_{m,1}\right| = \frac{1}{\sqrt{M}}$. (7) is simplified as

$$\max_{\mathbf{w}_k, \mathbf{f}_k^{rf}} \left\|\mathbf{w}_k^* \mathbf{H}_k \mathbf{f}_k^{rf}\right\| \tag{8}$$

It is very difficult, if not impossible, to solve the above non-convex optimization problem. In the following, we will perform the method of harvesting the large array gain of antenna to solve $\mathbf{w}_k$ and $\mathbf{f}_k^{rf}$ through the appropriate phase-only control at the RF domain. Note that no inter-user interference (IUI) is considered in solving the simplified maximization problem (8), which is a sub-optimal solution. The case with IUI can be investigated in future work.

We start with finding the optimal solution of $\mathbf{w}_k$ without respect to $\mathbf{f}_k^{rf}$. According to the principle of receiving the largest UE gain, for each UE, the design of the analogy combiner can be obtained by solving the following problem

$$\arg\max_{\mathbf{w}_k} \|\mathbf{w}_k^* \mathbf{H}_k\|_1^2 \tag{9}$$

In order to obtain the better solution of $\mathbf{w}_k$, we review the first two methods and propose the last two methods.

1) Exhaustive search method: Let us list all possible angles of analog precoding, and then get the vector sum of $\|\mathbf{w}_k^* \mathbf{H}_k\|_1^2$ with the knowledge of $\mathbf{H}_k$. The optimal angle of $\mathbf{w}_k$ to achieve the largest value can be determined. However, the biggest drawback of this method is that the possible types of precoder angels P are fixed. Furthermore, the computational complexity increases exponentially with M at the UE, which cannot be afforded when the number of antennas is large.

Algorithm 1 Hybrid Precoder Algorithm

Input: $\mathbf{w}_k$, $\mathbf{F}_{\mathrm{RF}}$.
Input: $\mathbf{H}$;
for $k \leq K$ **do**
  $\mathbf{H}_k = \mathbf{H}(k,:,:)$;
  $\mathbf{a}_k = \mathbf{a}_r(k,:,:)$;
  for $l \leq L_k$ **do**
    $\Phi(k,:) = \mathbf{a}_k^*(:,k) * \mathbf{H}_k$;
  end for
  $l = \arg\max_l \left| \left[\Phi\Phi^H\right]_{l,l} \right|$;
  $\mathbf{w}_k = \mathbf{a}_k(:,l)$;
  $\mathbf{F}_{\mathrm{RF}}(:,k) = \frac{1}{\sqrt{N}} e^{j\mathrm{angle}(\mathbf{w}_k^*\mathbf{H}_k)^*}$;
end for
Output: $\mathbf{F}_{\mathrm{BB}}$.
for $k \leq K$ **do**
  $\tilde{\mathbf{H}}_k = \mathbf{w}_k^*\mathbf{H}_k\mathbf{F}_{\mathrm{RF}}$;
  $\mathbf{H}_{eq}(k,:) = \tilde{\mathbf{H}}_k$;
end for
$\mathbf{F}_{\mathrm{BB}} = \mathbf{H}_{eq}\left(\mathbf{H}_{eq}\mathbf{H}_{eq}^H\right)^{-1}$.

2) DFT-based method: The vector path, which is the most relevant to $\mathbf{H}_k$, can be found in a DFT basis set $\mathcal{A}$ as

$$\begin{aligned} &\arg\max_{\mathbf{w}_k} \|\mathbf{w}_k^*\mathbf{H}_k\|_1^2 \\ &\text{s.t.} \qquad \mathbf{w}_k \in \mathcal{A}, \end{aligned} \tag{10}$$

where $\mathcal{A} = \left\{\mathbf{a}(0), \mathbf{a}\left(\frac{2\pi}{M}\right), \ldots, \mathbf{a}\left(\frac{2\pi(M-1)}{M}\right)\right\}$ is the DFT basis set from which the $\mathbf{w}_k$ is chosen. The disadvantage lies in the same direction angles of all antennas [16].

3) Correlation-based method: In the correlation-based method, the UE obtains the path vector which has the highest correlation with the channel $\mathbf{H}_k$ in all path vectors. More specifically, we can derive the analogy combiner by solving

$$\begin{aligned} &\mathbf{w}_k = \arg\max_{\mathbf{a}_{r,l}} \left\| \mathbf{a}_{r,l}^*\mathbf{H}_k \right\|_1^2 \\ &\text{s.t. } \mathbf{a}_{r,l} \in \{\mathbf{a}_{r,1}, \ldots \mathbf{a}_{r,L_k}\}. \end{aligned} \tag{11}$$

The analogy combiner $\mathbf{w}_k$ can be designed by selecting the receive array response vectors that is most relevant to channel $\mathbf{H}_k$ from the set of $\{\mathbf{a}_{t,1}, \ldots \mathbf{a}_{t,L_k}\}$.

4) Sum-based method: The UE first calculates the sum of all path vectors $\sum_{l=1}^{L_k} \mathbf{a}_{r,l}$. Then, let the UE's analog combining takes the angle of sum vectors. Hence, $\mathbf{w}_k$ can be expressed as $\mathbf{w}_k = \frac{1}{\sqrt{M}} e^{j\mathrm{angle}\left(\sum_{l=1}^{L_k} \mathbf{a}_{r,l}\right)}$.

After obtaining $\mathbf{w}_k$, we evaluate $\mathbf{h}_{kr} = \mathbf{w}_k^*\mathbf{H}_k$ to derive the solution of $\mathbf{f}_k^{rf}$ as $\arg\max_{\mathbf{f}_k^{rf}} \left\| \mathbf{h}_{kr}\mathbf{f}_k^{rf} \right\|$. To maximize $\max_{\mathbf{f}_k^{rf}} \left\| \mathbf{h}_{kr}\mathbf{f}_k^{rf} \right\|$, we only need to let the phase of $\mathbf{f}_k^{rf}$ takes the conjugate transpose of $\mathbf{h}_{kr}$. Submitting $\mathbf{w}_k$ and $\mathbf{f}_k^{rf}$ into (7) and (8), we can derive the precoding vector $\mathbf{F}_{\mathrm{RF}}$ for the BS and the combiner vector $\mathbf{w}_k$ for each UE, respectively.

B. Digital Precoding Design

When the analog precoding $\mathbf{F}_{\mathrm{RF}}$ and $\mathbf{w}_k$ is fixed, the design of the digital precoding actually becomes a conventional precoding problem. Therefore, we can define an equivalent channel for the kth UE as

$$\tilde{\mathbf{H}}_k = \mathbf{w}_k^*\mathbf{H}_k\mathbf{F}_{\mathrm{RF}}. \tag{12}$$

To eliminate interference among UEs, the classical ZF digital precoding algorithm could be adopted [17]. The multiuser mmWave equivalent channel $\mathbf{H}_{eq}$ can be described as $\mathbf{H}_{eq} = \left[\ \tilde{\mathbf{H}}_1, \tilde{\mathbf{H}}_2, \cdots, \tilde{\mathbf{H}}_K\ \right]^T$. Hence, the equivalent multiuser digital precoding $\mathbf{F}_{\mathrm{BB}}$ is given by $\mathbf{F}_{\mathrm{BB}} = \mathbf{H}_{eq}\left(\mathbf{H}_{eq}\mathbf{H}_{eq}^H\right)^{-1}$. For the k-th UE, we can directly get the digital precoding as $\mathbf{f}_{bb} = \tilde{\mathbf{H}}_k^H\left(\tilde{\mathbf{H}}_k\tilde{\mathbf{H}}_k^H\right)^{-1}$. To sum up, the pseudo-code of quantized hybrid precoding scheme is described in Algorithm 1.

IV. Achievable Rate Analysis

In this section, we derive the achievable rate expressions of mmWave multiuser massive MIMO systems with one- and multi-bit DACs. We start with 1-bit quantized hybrid precoder.

A. 1-bit Quantized Hybrid Precoder

As Bussgang theorem illustrates the cross correlation of a Gaussian signal before and after it has passed through a nonlinear operation [12], using it, the 1-bit DACs quantization operation as symmetric uniform quantizers is modeled here. We assume the digital signal s is Gaussian RVs, and the input signal of the quantization function can be considered as Gaussian as well. It allows us to decompose the quantized signal into two parts: a linear function of the input vector $\mathbf{x}_{\mathrm{H}} \triangleq \mathbf{F}_{\mathrm{BB}}\mathbf{s}$ and an output distortion term $\mathbf{d}$ uncorrelated with $\mathbf{x}_{\mathrm{H}}$. Thus, we have

$$\mathbf{x}_{\mathrm{L}} \triangleq \mathcal{Q}_{\mathrm{Bussgang}}(\mathbf{x}_{\mathrm{H}}) = \mathbf{G}\mathbf{x}_{\mathrm{H}} + \mathbf{d}, \tag{13}$$

where $\mathbf{G}$ is the quantization gains diagonal matrix and $\mathbf{d}$ denotes the quantization distortion vector uncorrelated with $\mathbf{x}_{\mathrm{H}}$. Note that the distortion $\mathbf{d}$ and the signal $\mathbf{s}$ are uncorrelated, e.g., $\mathbf{R}_{\mathbf{x}_{\mathrm{H}}\mathbf{d}} = \mathbf{R}_{\mathbf{d}\mathbf{x}_{\mathrm{H}}} = \mathbf{0}$ [18], [19]. Moreover, we have

$$\mathbf{R}_{\mathbf{x}_{\mathrm{L}}\mathbf{x}_{\mathrm{H}}} = \mathbf{G}\mathbf{R}_{\mathbf{x}_{\mathrm{H}}\mathbf{x}_{\mathrm{H}}} + \mathbf{R}_{\mathbf{d}\mathbf{x}_{\mathrm{H}}} = \mathbf{G}\mathbf{R}_{\mathbf{x}_{\mathrm{H}}\mathbf{x}_{\mathrm{H}}}, \tag{14}$$

where $\mathbf{R}_{\mathbf{x}_{\mathrm{H}}\mathbf{x}_{\mathrm{H}}} = \mathbf{F}_{\mathrm{BB}}\mathbf{F}_{\mathrm{BB}}^H$ denotes the auto-correlation matrix of $\mathbf{x}_{\mathrm{H}}$. By using classical arcsine law [20], we have

$$\mathbf{R}_{\mathbf{x}_{\mathrm{L}}\mathbf{x}_{\mathrm{L}}} = \frac{2}{\pi}\arcsin\left[\mathrm{diag}(\mathbf{R}_{\mathbf{x}_{\mathrm{H}}\mathbf{x}_{\mathrm{H}}})^{-\frac{1}{2}}\mathbf{R}_{\mathbf{x}_{\mathrm{H}}\mathbf{x}_{\mathrm{H}}}\mathrm{diag}(\mathbf{R}_{\mathbf{x}_{\mathrm{H}}\mathbf{x}_{\mathrm{H}}})^{-\frac{1}{2}}\right]. \tag{15}$$

Furthermore, the cross-correlation matrix $\mathbf{R}_{\mathbf{x}_{\mathrm{L}}\mathbf{x}_{\mathrm{H}}}$ between the input $\mathbf{x}_{\mathrm{L}}$ and output $\mathbf{x}_{\mathrm{H}}$ of the one-bit quantizer is obtained

$$\mathbf{R}_{\mathbf{x}_{\mathrm{L}}\mathbf{x}_{\mathrm{H}}} = \sqrt{\frac{2}{\pi}}\mathrm{diag}(\mathbf{R}_{\mathbf{x}_{\mathrm{H}}\mathbf{x}_{\mathrm{H}}})^{-\frac{1}{2}}\mathbf{R}_{\mathbf{x}_{\mathrm{H}}\mathbf{x}_{\mathrm{H}}}. \tag{16}$$

Substituting (14) into (16), we can obtain

$$\mathbf{G} = \sqrt{\frac{2}{\pi}}\mathrm{diag}\left(\mathbf{F}_{\mathrm{BB}}\mathbf{F}_{\mathrm{BB}}^H\right)^{-1/2}. \tag{17}$$

From (15) and (17), we can deduce the covariance matrix of the distortion $\mathbf{d}$ as

$$\begin{aligned} \mathbf{R}_{\mathbf{dd}} &= \mathbf{R}_{\mathbf{x}_{\mathrm{L}}\mathbf{x}_{\mathrm{L}}} - \mathbf{G}\mathbf{R}_{\mathbf{x}_{\mathrm{H}}\mathbf{x}_{\mathrm{H}}}\mathbf{G}^H \\ &\overset{(a)}{\approx} \frac{2}{\pi}\left[\arcsin\{\mathbf{I}_K\} - \mathbf{I}_K\right] = \frac{\pi-2}{\pi}\mathbf{I}_K \end{aligned} \tag{18}$$

where (a) is based on the fact that the digital precoder matrix $\mathbf{F}_{\mathrm{BB}}$ is a square matrix and the approximation equation $\mathbf{F}_{\mathrm{BB}}\mathbf{F}_{\mathrm{BB}}^H \approx \mathrm{diag}\left(\mathbf{F}_{\mathrm{BB}}\mathbf{F}_{\mathrm{BB}}^H\right)$ [21].

Using (13) and (17), (3) can be rewritten as

$$r_k^B = \tilde{\mathbf{H}}_k \mathbf{G}\mathbf{f}_k^{bb} s_k + \sum_{u\neq k}^{K} \tilde{\mathbf{H}}_k \mathbf{G}\mathbf{f}_u^{bb} s_u + \tilde{\mathbf{H}}_k \mathbf{d} + \mathbf{w}_k^* \mathbf{n}_k. \quad (19)$$

According to (5), the achievable rate R_k for the kth UE is given by $R_k = \log_2\left(1+\mathrm{SIDNR}_k^B\right)$, where the signal-to-interference-noise-and-distortion ratio (SIDNR) at the kth UE is expressed as

$$\mathrm{SIDNR}_k^B = \frac{\left|\tilde{\mathbf{H}}_k \mathbf{G}\mathbf{f}_k^{bb} s_k\right|^2}{\sum\limits_{u\neq k}^{K}\left|\tilde{\mathbf{H}}_k \mathbf{G}\mathbf{f}_u^{bb} s_u\right|^2 + \left|\tilde{\mathbf{H}}_k \mathbf{d}\right|^2 + \left|\mathbf{w}_k^* \mathbf{n}_k\right|^2}. \quad (20)$$

B. Multi-bit Quantized Hybrid Precoder

As AQNM is a special model of Bussgang theorem, we will adopt the AQNM to decompose the quantized signal into two parts: a linear function of the input $\mathbf{x}_{\mathrm{H}}$ to the quantizers and a distortion term that is uncorrelated with the input to the quantizers [22]–[24]. Thus the quantized output vector can be decomposed as

$$\mathcal{Q}_{\mathrm{AQNM}}\left(\mathbf{x}_{\mathrm{H}}\right) = (1-\eta)\,\mathbf{F}_{\mathrm{BB}}\mathbf{s} + \mathbf{q}, \quad (21)$$

where η is the quantization distortion factor for multi-bits DAC and $\mathbf{q}$ denotes the quantization distortion vector uncorrelated with $\mathbf{F}_{\mathrm{BB}}$. Note that the quantization error can be well approximated as a linear gain with AQNM, and we can deduce the covariance matrix of the distortion $\mathbf{q}$ as

$$\mathbf{R}_{\mathbf{qq}} = \eta(1-\eta)\mathrm{diag}(\mathbf{F}_{\mathrm{BB}}\mathbf{F}_{\mathrm{BB}}^H). \quad (22)$$

Using (21), we can derive

$$r_k^A = (1-\eta)\left(\tilde{\mathbf{H}}_k \mathbf{f}_k^{bb} s_k + \sum_{u\neq k}^{K} \tilde{\mathbf{H}}_k \mathbf{f}_u^{bb} s_u\right) + \tilde{\mathbf{H}}_k \mathbf{q} + \mathbf{w}_k^* \mathbf{n}_k. \quad (23)$$

According to (5), the achievable rate R_k for the kth UE can be expressed as $R_k = \log_2\left(1+\mathrm{SIDNR}_k^A\right)$, where

$$\mathrm{SIDNR}_k^A = \frac{(1-\eta)^2\left|\tilde{\mathbf{H}}_k \mathbf{f}_k^{bb} s_k\right|^2}{(1-\eta)^2\sum\limits_{u\neq k}^{K}\left|\tilde{\mathbf{H}}_k \mathbf{f}_u^{bb} s_u\right|^2 + \left|\tilde{\mathbf{H}}_k \mathbf{q}\right|^2 + \left|\mathbf{w}_k^* \mathbf{n}_k\right|^2}. \quad (24)$$

For one-bit quantization, the exact distortion factor $\eta = 1 - 2/\pi = 0.3634$; for two-bit quantization, we have $\eta = 0.1175$; for other quantization bits (e.g., the number of bits $n > 2$), the distortion factors can be approximated as $\eta \approx \frac{\pi\sqrt{3}}{2}2^{-2b}$ [24].

V. Numerical Results

In this section, we present the results of numerical simulations conducted to evaluate the effects of low-resolution DACs on the multi-user mmWave massive hybrid precoding system. The propagation path between the BS and the kth UE are generated as $L_k = 3$. The gain of the propagation path $\alpha_{k,l}$ is assumed to be i.i.d. Gaussian RVs with zero mean and unit variance. The antenna elements are set to be the uniform linear array for simplicity. The azimuths are assumed to be uniformly distributed in $[0, 2\pi]$. In the simulation, the obtained results are averaged over 200 independent channel realizations.

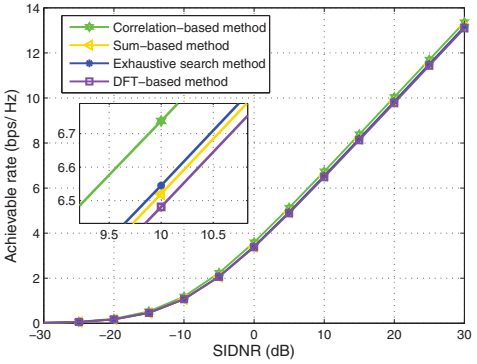

Fig. 2. Achievable rate of UE with different quantized hybrid precoding algorithms ($N = 64$, $M = 4$, and $K = 8$).

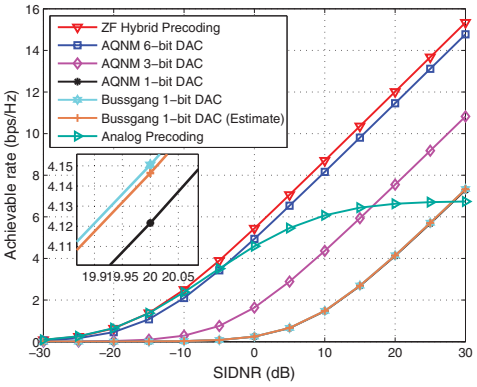

Fig. 3. Achievable rate of UE with different low-resolution DACs ($N = 128$, $M = 8$, and $K = 8$).

Figure 2 plots average achievable rate of UE achieved by different quantized hybrid precoding algorithms. It is clear to see that the achievable rate increases with the SIDNR. Moreover, numerical results demonstrate that the correlation-based method can achieve the best rate performance than other methods. This is due to the fact that when the selected path vector and the channel matrix are highly correlated, the gain from the analogy combiner at the UE is increased. Due to the low complexity and high performance, in the following figures, we use the correlation-based method.

Figure 3 shows the achievable rate of UE against different SIDNRs in mmWave multiuser massive MIMO systems with low-resolution DACs at the BS. First, we find that employing one-bit DACs severely degrades the rate performance due to large quantization errors. Moreover, the exact curve of 1-bit DAC with Bussgang and its approximated curve coincide with each other, which validates the accuracy of the approximation (18). Fig. 3 also validates the common belief that the quantization distortion is negligible at low SIDNR even with low-resolution DACs at the BS. With the increase of bits,

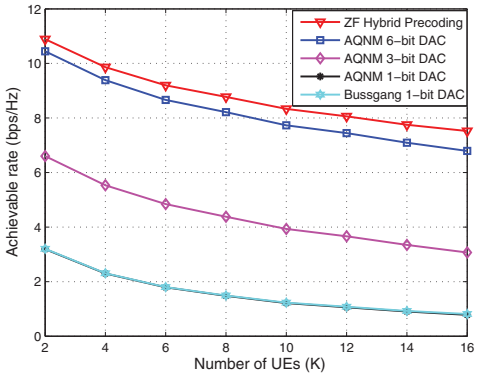

Fig. 4. Achievable rate of UE against the number of UEs ($N = 128$, $M = 8$, and SNR=10 dB).

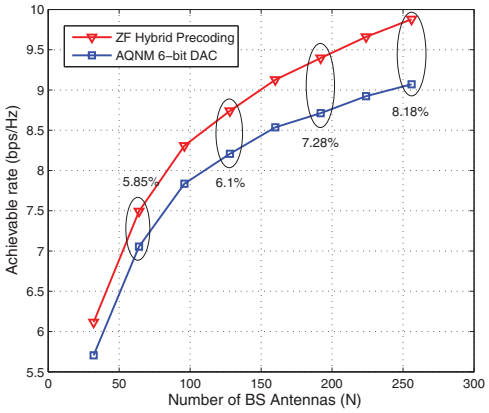

Fig. 5. Achievable rate of UE against the number of BS antennas ($M = 8$, $K = 8$, and SNR = 10 dB).

the achievable rate also increases. However, one can obtain a considerable performance with only 6-bit DACs in the quantized mmWave multiuser massive MIMO system.

The effects of the number of UEs and BS antennas on the achievable rate are investigated in Figs. 4 and 5, respectively. In Fig. 4, we find that adding the number of UEs can significantly reduce the average achievable rate due to inter-user interference. On the contrary, the system can achieve superior performance if a large number of BS antennas can be deployed. However, the gap between the ideal and quantized hybrid precoding algorithms becomes large as the number of BS antennas increases.

VI. Conclusion

We propose a low-complexity hybrid precoding method for the mmWave multiuser MIMO system with low-resolution DACs. More specifically, the correlation based method can maximize the analogy combiner gain, and the ZF precoding is utilized to mitigate the interference among UEs. To provide an approximate linear representation of quantization noise, the Bussgang theorem and the AQNM are adopted for 1-bit DACs and multi-bit DACs, respectively. Our results indicated that the proposed quantized precoding method can significantly reduce the complexity and achieve a considerable rate performance.

References

[1] T. L. Marzetta, "Noncooperative cellular wireless with unlimited numbers of base station antennas," *IEEE Trans. Wireless Commun.*, vol. 9, no. 11, pp. 3590–3600, Nov. 2010.

[2] J. Zhang, E. Björnson, M. Matthaiou, D. W. K. Ng, H. Yang, and D. J. Love, "Multiple antenna technologies for beyond 5G," *arXiv:1910.00092*, 2019.

[3] D. W. K. Ng, E. S. Lo, and R. Schober, "Energy-efficient resource allocation in OFDMA systems with large numbers of base station antennas," *IEEE Trans. Wireless Commun.*, vol. 11, no. 9, pp. 3292–3304, Sep. 2012.

[4] X. Wei, L. Xiang, L. Cottatellucci, T. Jiang, and R. Schober, "Cache-aided massive MIMO: Linear precoding design and performance analysis," in *Proc. IEEE ICC*, 2019, pp. 1–7.

[5] J. Zhang, L. Dai, X. Li, Y. Liu, and L. Hanzo, "On low-resolution ADCs in practical 5G millimeter-wave massive MIMO systems," *IEEE Commun. Mag.*, vol. 56, no. 7, pp. 205–211, Jul. 2018.

[6] J. Zhang, L. Dai, Z. He, B. Ai, and O. A. Dobre, "Mixed-ADC/DAC multipair massive MIMO relaying systems: Performance analysis and power optimization," *IEEE Trans. Commun.*, vol. 67, no. 1, pp. 140–153, Jan. 2018.

[7] J. Zhang, J. Zhang, and B. Ai, "Cell-free massive MIMO with low-resolution ADCs over spatially correlated channels," *in Proc. IEEE ICC*, pp. 1–6, Jun. 2020.

[8] J. Xu, W. Xu, and F. Gong, "On performance of quantized transceiver in multiuser massive MIMO downlinks," *IEEE Wireless Commun. Lett.*, vol. 6, no. 5, pp. 562–565, Oct. 2017.

[9] L. N. Ribeiro, S. Schwarz, M. Rupp *et al.*, "Energy efficiency of mmWave massive MIMO precoding with low-resolution DACs," *IEEE J. Sel. Topics Signal Process.*, vol. 12, no. 2, pp. 201–211, Feb. 2018.

[10] M. Shao, Q. Li, and W.-K. Ma, "One-bit massive MIMO precoding via a minimum symbol-error probability design," *in Proc. IEEE ICASSP*, pp. 3579–3583, 2018.

[11] S. Jacobsson, G. Durisi, M. Coldrey, T. Goldstein, and C. Studer, "Quantized precoding for massive MU-MIMO," *IEEE Trans. Commun.*, vol. 65, no. 11, pp. 4670–4684, Nov. 2017.

[12] S. Han, I. Chih-Lin, Z. Xu, and C. Rowell, "Large-scale antenna systems with hybrid analog and digital beamforming for millimeter wave 5G," *IEEE Commun. Mag.*, vol. 53, no. 1, pp. 186–194, Jan. 2015.

[13] A. F. Molisch, V. V. Ratnam, S. Han, Z. Li, S. L. H. Nguyen, L. Li, and K. Haneda, "Hybrid beamforming for massive MIMO: A survey," *IEEE Commun. Mag.*, vol. 55, no. 9, pp. 134–141, Sep. 2017.

[14] A. Alkhateeb, G. Leus, and R. W. Heath, "Limited feedback hybrid precoding for multi-user millimeter wave systems," *IEEE Trans. Wireless Commun.*, vol. 14, no. 11, pp. 6481–6494, Nov. 2015.

[15] O. El Ayach, S. Rajagopal, S. Abu-Surra, and Z. Pi, "Spatially sparse precoding in millimeter wave MIMO systems," *IEEE Trans. Wireless Commun.*, vol. 13, no. 3, pp. 1499–1513, Mar. 2014.

[16] W. Ni and X. Dong, "Hybrid block diagonalization for massive multiuser MIMO systems," *IEEE Trans. Wireless Commun.*, vol. 64, no. 1, pp. 201–211, Jan. 2016.

[17] L. Liang, W. Xu, and X. Dong, "Low-complexity hybrid precoding in massive multiuser MIMO systems," *IEEE Wireless Commun. Lett.*, vol. 3, no. 6, pp. 653–656, Jun. 2014.

[18] S. Jacobsson, G. Durisi, M. Coldrey, T. Goldstein, and C. Studer, "Quantized precoding for massive MU-MIMO," *IEEE Trans. Commun.*, vol. 65, no. 11, pp. 4670–4684, Jul. 2017.

[19] A. K. Saxena, I. Fijalkow, and A. L. Swindlehurst, "Analysis of one-bit quantized precoding for the multiuser massive MIMO downlink," *IEEE Trans. Signal Process.*, vol. 65, no. 17, pp. 4624–4634, Sep. 2017.

[20] A. Papoulis and S. U. Pillai, *Probability, Random Variables, and Stochastic Processes*. Tata McGraw-Hill Education, 2002.

[21] C. Kong, A. Mezghani, C. Zhong, A. L. Swindlehurst, and Z. Zhang, "Multipair massive MIMO relaying systems with one-bit ADCs and DACs," *IEEE Trans. Signal Process.*, vol. 66, no. 11, pp. 2984–2997, Nov. 2018.

[22] J. Mo, A. Alkhateeb, S. Abu-Surra, and R. W. Heath, "Hybrid architectures with few-bit ADC receivers: Achievable rates and energy-rate tradeoffs," *IEEE Trans. Wireless Commun.*, vol. 16, no. 4, pp. 2274–2287, Apr. 2017.

[23] J. Zhang, L. Dai, Z. He, S. Jin, and X. Li, "Performance analysis of Mixed-ADC massive MIMO systems over Rician fading channels," *IEEE J. Sel. Areas Commun.*, vol. 35, no. 6, pp. 1327–1338, Jun. 2017.

[24] J. Zhang, L. Dai, S. Sun, and Z. Wang, "On the spectral efficiency of massive MIMO systems with low-resolution ADCs," *IEEE Commun. Lett.*, vol. 20, no. 5, pp. 842–845, May 2016.